

# RSC Advances



This is an *Accepted Manuscript*, which has been through the Royal Society of Chemistry peer review process and has been accepted for publication.

*Accepted Manuscripts* are published online shortly after acceptance, before technical editing, formatting and proof reading. Using this free service, authors can make their results available to the community, in citable form, before we publish the edited article. This *Accepted Manuscript* will be replaced by the edited, formatted and paginated article as soon as this is available.

You can find more information about *Accepted Manuscripts* in the [Information for Authors](#).

Please note that technical editing may introduce minor changes to the text and/or graphics, which may alter content. The journal's standard [Terms & Conditions](#) and the [Ethical guidelines](#) still apply. In no event shall the Royal Society of Chemistry be held responsible for any errors or omissions in this *Accepted Manuscript* or any consequences arising from the use of any information it contains.

# Two-Bit-Per-Cell Resistive Switching Memory Device With Ti/MgZnO/Pt Structure

Wei-Kang Hsieh, Ricky W. Chuang\*, Shouu-Jinn Chang

<sup>1</sup>Institute of Microelectronics and Department of Electrical Engineering, Advanced Optoelectronic Technology Center, National Cheng Kung University, Tainan 70101, Taiwan

\*e-mail: [rwchuang@mail.ncku.edu.tw](mailto:rwchuang@mail.ncku.edu.tw)

## Abstract

We report the fabrication and characterization of resistive random access memory (RRAM) with Ti/MgZnO/Pt structure at room temperature. Four different resistive states are obtained by applying different stop voltages ( $V_{\text{stop}}$ ) for the reset process. These four resistance states show good retention characteristics without any degradation and can be clearly distinguished from one another by more than 10,000 second under 100mV stress. The current transport mechanism is dictated by a Schottky emission as the stop voltage  $V_{\text{stop}}$  increases from 1 to 1.5 V. The mechanism of multilevel RS is investigated and band diagrams are used to explain the multilevel RS phenomenon associated with Ti/MgZnO/Pt based RRAM devices.

## Introduction

With an increasing demand for the portable electronic products nowadays in our daily life, as one of vital components, the need for the nonvolatile memory (NVM) has also climbed up accordingly. However, with the device feature size continuously shrinking, the conventional floating-gate NVM has confronted several technical and physical limitations [1],[2]. To overcome this issue, resistive random access memory (RRAM) appears to be a viable solution [3],[4]. As one of the suitable candidates, RRAM has various advantages, such as low power consumption, simple structure, high integration density and fast operation speed [5],[6]. To further enhance the performances of RRAM, devices with multilevel characteristics have been developed to increase the bit density but with the cost per bit reduced [7],[6]. It is known that binary transition metal oxides used in RRAM application exhibit high write/erase speed, high storage density, and are compatible with semiconductor integration circuits [9], such as  $\text{TiO}_2$  [10],  $\text{TaO}_x$  [11],  $\text{NiO}$ , and  $\text{VO}_2$  [12]. Among these candidates, ZnO-based films have emerged as the promising material for RRAM application owing to their superior resistive switching capabilities, including the switching speed achieved at the nanosecond level, naturally transparent in their own right and multilevel characteristics performance [13],[14],[15].

As one of the ZnO-based materials, MgZnO has been well recognized in optoelectronic device applications [16],[17]. Furthermore, the high performance/cost RRAM can be achieved because of its abundant availability, low cost, well known manufacture process, and others. Therefore, MgZnO-based RRAM deserves to be investigated extensively in light of the aforementioned merits.

In this work, we report a simple memory device that incorporates a Ti/MgZnO/Pt structure and the corresponding current-voltage ( $I$ - $V$ ) characteristics are evaluated. We

seek to demonstrate the multilevel switching can be realized based on the movement of the oxygen vacancies in MgZnO by controlling the stop voltage ( $V_{\text{stop}}$ ) of the reset process.

## Experimental

The sandwiched structure of the RRAM device utilized in this study is shown schematically in Fig. 1. To fabricate the structure, a 10-nm-thick Ti is first deposited onto a chemically cleaned glass substrate to serve as the adhesion layer by e-beam evaporation system. A 40-nm-thick Pt layer is then e-beam evaporated to serve as the bottom electrode (BE). Subsequently, a 20-nm-thick MgZnO thin film is deposited by RF sputtering the  $\text{Mg}_{0.1}\text{Zn}_{0.9}\text{O}$  target in mixed argon and oxygen ambient at room temperature. During the sputtering process, the RF power and chamber pressure are kept at 80 W and 10 mTorr, respectively. Finally, a 100-nm-thick Ti layer is then deposited onto the sputtered MgZnO thin film to serve as the top electrode (TE) with a size of  $50 \times 50 \mu\text{m}$  by e-beam evaporation. The resistive switching behaviors of the fabricated devices are investigated by characterizing the current-voltage ( $I$ - $V$ ) curves through voltage scanning mode using Agilent B1500a semiconductor parameter analyzer. During these  $I$ - $V$  measurements, the bias voltage is applied onto the Ti TE while the Pt BE is remained electrically grounded.

## Results and discussion

Initially, a negative bias is applied to the device to investigate the  $I$ - $V$  characteristic. At this operating point, a large current density is obtained which indicates that the conduction filaments have already been existed in the device. After adding a sufficiently large positive bias, the device switches from a low resistance stage (LRS) to a high resistance stage (HRS), or the reset process. Subsequently, if an adequate negative voltage is applied, the device then turns from HRS to LRS, or the set process. The fabricated RRAM exhibits a uniform bipolar resistive switching (BRS), in which the opposite voltage polarity is needed to activate/deactivate the conductive filaments [5]. Moreover, the device is investigated to ensure the multilevel operation is achieved by controlling the stop voltage ( $V_{\text{stop}}$ ), as shown in Fig. 2(a). First, a  $V_{\text{stop}}$  equalled to 1 V is applied to the TE. During this operation process, the device is reset at about 0.6V, corresponding to the the reset voltage ( $V_{\text{reset}}$ ). When a negative voltage of  $-1.5$  V is applied, the RRAM switches from HRS to LRS at about  $-0.75$  V, corresponding to the set voltage ( $V_{\text{set}}$ ). By following this  $I$ - $V$  operation sequence,  $0$  V  $\rightarrow$   $+V_{\text{stop}}$   $\rightarrow$   $0$  V  $\rightarrow$   $-1.5$  V  $\rightarrow$   $0$ V, with different  $V_{\text{stop}}$  applied, namely, 1 V, 1.2 V and 1.5 V, a significant change in the magnitude of HRS current is observed as the  $V_{\text{stop}}$  is varied. In addition, four distinct states accompanying with the LRS is observed, which are conveniently labelled as 00, 01, 10, and 11, respectively. Fig. 2(b) shows the retentions of the LRS (11) and HRS (00, 01, 10 states). The resistance values of these four states are measured at 100 mV at room temperature. After 10,000s, it is found that the four states can be clearly distinguished without retention degradation. Furthermore, the endurance characteristic of the fabricated RRAM device is evaluated in DC sweep measurement mode with a result shown in Fig. 2(c). It can also be found that there are four states with a reading voltage of

100mV without any operational errors. According to the results of data retention and endurance tests gathered, the Ti/MgZnO/Pt device appears to be suitable for multilevel application.

The switching stability test is performed based on the cycle-to-cycle measurement mode [18],[19]. With 500 successive switching cycles applied to a single device, a statistical analysis can thus be made in order to acquire further information on the switching stability, and the results are successively shown in Fig. 3. In Fig. 3(a), cumulative probabilities of the resistance in these four states are calculated. It can be found that these four states do not overlap with one another, thereby avoiding the possible failure of data storage. Note that the resistances of these four states extend to a certain extent during a cycling measurement, especially for higher resistance states. In Fig. 3(b), statistical analysis of the set and reset voltages for three different stop voltage is performed. For  $V_{\text{reset}}$ , it remains stable regardless of the enlargement of  $V_{\text{stop}}$ . On the contrary,  $V_{\text{set}}$  is observed to slightly increase with the enlargement of  $V_{\text{stop}}$ . Owing to the larger  $V_{\text{stop}}$  or a larger strength of electric field applied, the filaments become more vigorously disrupted. Consequently, a larger  $V_{\text{set}}$  is even needed to reconnect the conduction filaments back together so that the device can be switched back to LRS.

To clarify the switching mechanism associated with these three HRSs,  $I$ - $V$  curves of these three HRSs obtained earlier are replotted and curve-fitted in order to analyze the carrier transport, as shown in Fig. 4. As shown in Fig. 4(a), the part of the HRS curve just undergo a transition from LRS curve is taken into analysis for each stop voltage, each of which is respectively shown in b thru d. The  $I$ - $V$  fitting corresponding to  $V_{\text{stop}} = 1$  V indicates that the current conduction involved in the HRS is dominated by the Schottky emission, as shown in Fig. 4(b). As  $V_{\text{stop}}$  becomes 1.2V, as shown in Fig. 4(c),  $\ln(I)$  is found to be linearly depended on  $V^{1/2}$ . Such a result suggests that the

current transport is also dominated by Schottky emission [7]. When  $V_{\text{stop}} = 1.5\text{V}$ , the result depicted in Fig. 4(d) reveals that  $\ln(I)$  is a function of  $V^{1/2}$ , indicating that the current transport is clearly dictated by Schottky emission again.

In order to further elaborate the aforementioned conduction mechanisms involved, the corresponding carrier transport mechanisms are presented in a diagrammatic manner in order to explain the resistive switching characteristic, as shown in Fig. 5. Usually, Ti is easily formed as a thin  $\text{TiO}_x$  layer at the Ti/oxide interface [20]. In this report, the enthalpy with O atom for Ti, Mg, and Zn are  $-994$  kJ/mol,  $-601$  kJ/mol, and  $-350$  kJ/mol, respectively [21]. Hence, Ti will preferentially bond with O atoms which are diffused from MgZnO, and leaving behind a numerous oxygen vacancies in MgZnO. Initially, oxygen vacancy-based conductive filaments physically connect the TE with BE (Fig. 5(a)) and Ti/MgZnO/Pt RRAM device remains in LRS [22]. After applying a bias with  $V_{\text{stop}} = 1$  V, the oxygen vacancies initially present at the interface between Ti and MgZnO start to recede into MgZnO as propelled by the electric field coming from the bias. At this instance, the conduction path close to Ti interface is broken and a thin MgZnO layer starts to develop. Consequently, electrons emitted across the potential energy barrier between the thin MgZnO layer and Ti TE becomes a dominant carrier transport mechanism since the energy band bending is relatively insignificant. This result suggests that the conduction mechanism for the HRS of  $V_{\text{stop}} = 1\text{V}$  is in fact dominated by Schottky emission, as shown in Fig. 5(b). After the set process is activated, the RRAM returns to LRS again, as illustrated in Fig. 5(a). When,  $V_{\text{stop}}$  is increased from 1 to 1.2 V, more oxygen vacancies near the interface between Ti and MgZnO are expected to pull back into MgZnO owing to the presence of a larger electric field, rendering an increase in the thickness of the thin MgZnO layer previously formed near Ti interface. In fact, adding an additional 0.2 V only has a mild effect on band bending, making the carrier

emission mechanism associated with the HRS at  $V_{\text{stop}}=1.2$  V to remain Schottky, as illustrated in Fig. 5(c).. Once RRAM is returned to LRS and  $V_{\text{stop}}=1.5$  V is applied, an increasing amount of oxygen vacancies near the interface between Ti and MgZnO are driven back into MgZnO due to again a larger electric field because of increasing  $V_{\text{stop}}$ . That is to say, the thickness of the thin MgZnO layer formed near Ti interface and the band bending both are expected to augment in a substantial manner. However, the amount of increase in band bending is still far from sufficient to change the conduction mechanism, so that in the end the conduction mechanism for the HRS at  $V_{\text{stop}}=1.5$ V still remains Schottky-emitting in nature, as schematically illustrated in Fig. 5(d).

## Conclusion

The RRAM device with Ti/MgZnO/Pt sandwich structure is proposed and fabricated at room temperature, and its characteristics are characterized. In addition to the excellent bipolar resistive switching characteristics obtained, the RRAM device exhibits a robust retention of four multilevel, which means 2 bits storage applications can be readily realized. From the analysis of the  $I$ - $V$  measurements, it is found that the current conduction associate with the HRS state is dominated by Schottky emission as the  $V_{\text{stop}}$  increases from 1 to 1.5V. This simple Ti/MgZnO/Pt bipolar RRAM device with four multilevel provides the applicable solution to the storage enlargement of the memory per cell.

## Reference

- [1] D. Jiang, M. Zhang, Z. Huo, *et al.*, “A study of cycling induced degradation mechanisms in Si nanocrystal memory devices,” *Nanotechnology*, vol. 22, pp. 254009-254001-254009-254005, Jun 24 2011.
- [2] C. Zhu, Z. Xu, Z. Huo, *et al.*, “Investigation on interface related charge trap and loss characteristics of high-k based trapping structures by electrostatic force microscopy,” *Appl. Phys. Lett.*, vol. 99, pp. 223504-223501-223504-223503, Nov 28 2011.
- [3] F. Pan, S. Gao, C. Chen, *et al.*, “Recent progress in resistive random access memories: Materials, switching mechanisms, and performance,” *Materials Science & Engineering R-Reports*, vol. 83, pp. 1-59, Sep 2014.
- [4] H. S. P. Wong, H. Y. Lee, S. Yu, *et al.*, “Metal-Oxide RRAM,” *Proc. IEEE*, vol. 100, pp. 1951-1970, Jun 2012.
- [5] W. K. Hsieh, K. T. Lam, and S. J. Chang, “Characteristics of tantalum-doped silicon oxide-based resistive random access memory,” *Mat. Sci. Semicon. Proc.*, vol. 27, pp. 293-296, Nov 2014.
- [6] R. Waser and M. Aono, “Nanoionics-based resistive switching memories,” *Nature Mater.*, vol. 6, pp. 833-840, Nov 2007.
- [7] W. K. Hsieh, K. T. Lam, and S. J. Chang, “Bipolar Ni/ZnO/HfO<sub>2</sub>/Ni RRAM with multilevel characteristic by different reset bias,” *Mat. Sci. Semicon. Proc.*, vol. 35, pp. 30-33, Jul 2015.
- [8] S. Yu and H.-S. P. Wong, “Compact modeling of conducting-bridge random-access memory (CBRAM),” *IEEE T. Electron Dev.*, vol. 58, pp. 1352-1360, 2011.
- [9] Y. H. Tseng, C. E. Huang, C. Kuo, *et al.*, “High density and ultra small cell size of contact ReRAM (CR-RAM) in 90nm CMOS logic technology and circuits,” in *IEDM Tech. Dig.*, 2009, pp. 1-4.
- [10] W. Y. Chang, Y. T. Ho, T. C. Hsu, *et al.*, “Influence of crystalline constituent on resistive switching properties of TiO<sub>2</sub> memory films,” *Electrochem. Solid State Lett.*, vol. 12, pp. H135-H137, 2009.
- [11] S. Maikap, D. Jana, M. Dutta, *et al.*, “Self-compliance RRAM characteristics using a novel W/TaO<sub>x</sub>/TiN structure,” *Nanoscale Res. Lett.*, vol. 9, pp. 292, Jun 10 2014.
- [12] M. J. Lee, Y. Park, D. S. Suh, *et al.*, “Two series oxide resistors applicable to high speed and high density nonvolatile memory,” *Adv. Mater.*, vol. 19, pp. 3919-3923, 2007.

- [13] S. Kim, H. Moon, D. Gupta, *et al.*, “Resistive, Switching Characteristics of Sol-Gel Zinc Oxide Films for Flexible Memory Applications,” *IEEE T. Electron Dev.*, vol. 56, pp. 696-699, Apr 2009.
- [14] C. C. Shih, K. C. Chang, T. C. Chang, *et al.*, “Resistive Switching Modification by Ultraviolet Illumination in Transparent Electrode Resistive Random Access Memory,” *IEEE Electron Device Lett.*, vol. 35, pp. 633-635, Jun 2014.
- [15] S. M. Lin, J. Y. Tseng, T. Y. Su, *et al.*, “Tunable Multilevel Storage of Complementary Resistive Switching on Single-Step Formation of ZnO/ZnWO<sub>x</sub> Bilayer Structure via Interfacial Engineering,” *Acs Appl. Mater. Inter.*, vol. 6, pp. 17686-17693, Oct 22 2014.
- [16] J. Y. Li, S. P. Chang, H. H. Lin, *et al.*, “High Responsivity Mg<sub>x</sub>Zn<sub>1-x</sub>O Film UV Photodetector Grown by RF Sputtering,” *IEEE Phontic Tech. L.*, vol. 27, pp. 978-981, May 1 2015.
- [17] T. H. Wu, I. C. Cheng, C. C. Hsu, *et al.*, “UV photocurrent responses of ZnO and MgZnO/ZnO processed by atmospheric pressure plasma jets,” *J. Alloy Compd.*, vol. 628, pp. 68-74, Apr 15 2015.
- [18] S. Gao, C. Song, C. Chen, *et al.*, “Dynamic Processes of Resistive Switching in Metallic Filament-Based Organic Memory Devices,” *J. Phys. Chem. C*, vol. 116, pp. 17955-17959, Aug 23 2012.
- [19] S. Gao, F. Zeng, F. Li, *et al.*, “Forming-free and self-rectifying resistive switching of the simple Pt/TaO<sub>x</sub>/n-Si structure for access device-free high-density memory application,” *Nanoscale*, vol. 7, pp. 6031-6038, 2015 2015.
- [20] D. Panda, C. Y. Huang, and T. Y. Tseng, “Resistive switching characteristics of nickel silicide layer embedded HfO<sub>2</sub> film,” *Appl. Phys. Lett.*, vol. 100, pp. 112901-112901-112901-112905, Mar 12 2012.
- [21] Y. Hou, Z. Mei, H. Liang, *et al.*, “Annealing Effects of Ti/Au Contact on n-MgZnO/p-Si Ultraviolet-B Photodetectors,” *IEEE T. Electron Dev.*, vol. 60, pp. 3474-3477, Oct 2013.
- [22] X. M. Chen, W. Hu, S. X. Wu, *et al.*, “Complementary switching on TiN/MgZnO/ZnO/Pt bipolar memory devices for nanocrossbar arrays,” *J. Alloy Compd.*, vol. 615, pp. 566-568, 5 Dec. 2014.

## Figure Captions

Fig. 1 The schematic diagram showing the fabricated Ti/MgZnO/Pt RRAM device ready for measurement.

Fig. 2 (a) The I-V curve of the Ti/MgZnO/Pt cell evaluated with different stop voltages ( $V_{\text{stop}}$ ) applied. (b) Retention characteristics of four resistive states measurement conducted at room temperature. (c) A switching cycle test that involves the measurement of the four resistive states at room temperature.

Fig. 3 (a) Cumulative probabilities of resistance associated with the four resistive states. (b) The distributions of  $V_{\text{set}}$  and  $V_{\text{reset}}$  as function of different  $V_{\text{stop}}$  voltages.

Fig. 4 (a) Parts of the  $IV$  curves are isolated for curve fitting for the purpose of extracting the pertinent carrier transport parameters associated with the different  $V_{\text{stop}}$ . The results of curve fitting are shown in (b), (c) and (d) which corresponds individually to the same plotting symbols used in (a)

Fig. 5 The schematic diagrams for describing different carrier conduction mechanisms involved for the proposed Ti/MgZnO/Pt RRAM device: (a) initial state and LRS, (b)  $V_{\text{stop}} = 1$  V, (c)  $V_{\text{stop}} = 1.2$  V, and (d)  $V_{\text{stop}} = 1.5$  V.

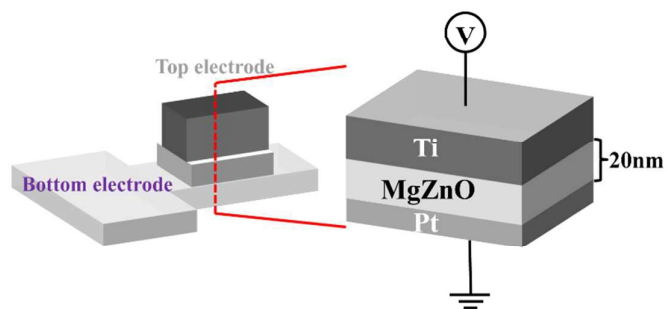


Fig. 1

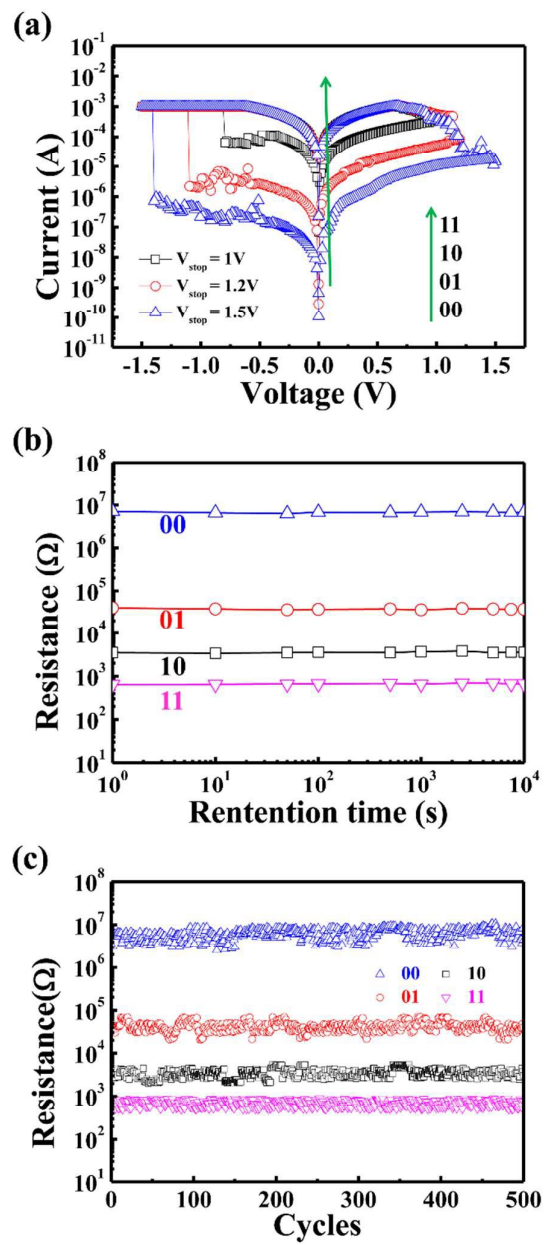


Fig. 2

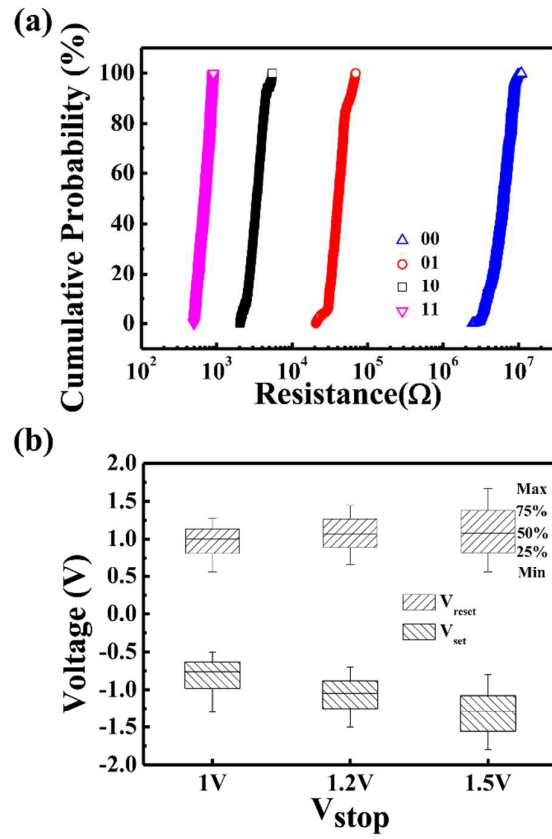


Fig. 3

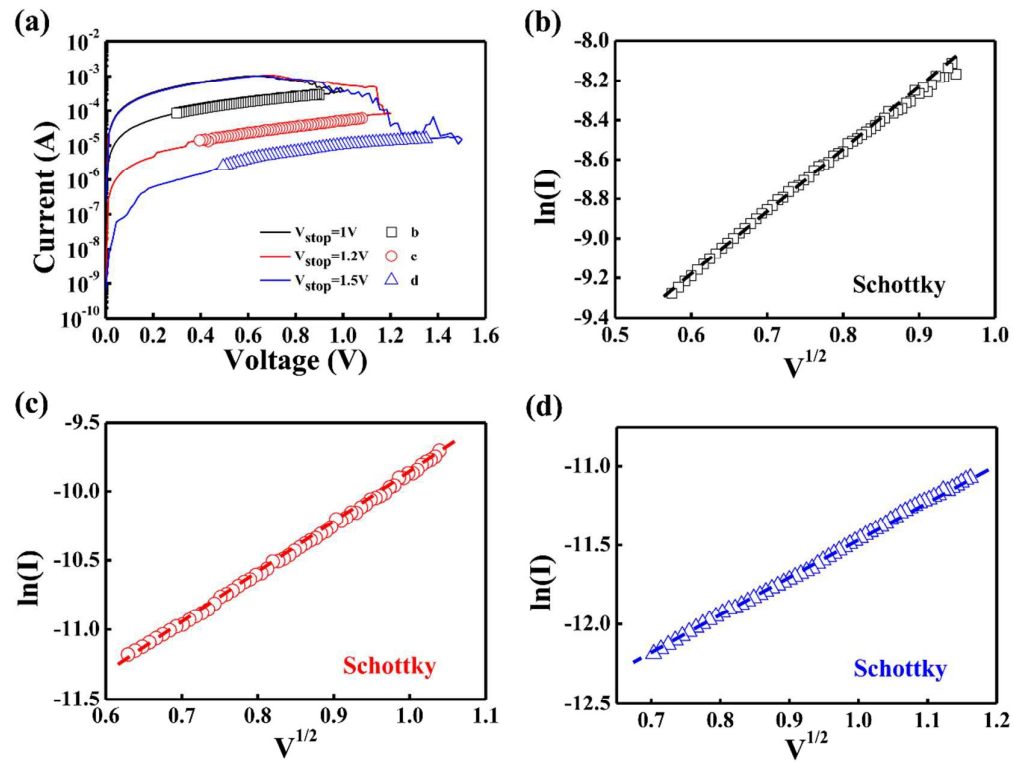


Fig. 4

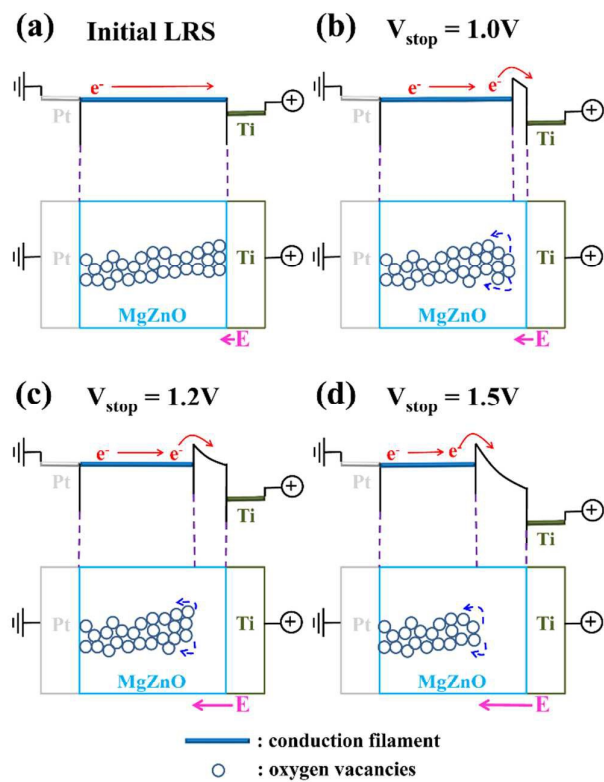


Fig. 5